Climate Dynamics
https://doi.org/10.1007/s00382-024-07150-0

ORIGINAL ARTICLE

Extreme dry advection dominates the record-breaking Yangtze River heatwave in midsummer of 2022

Shuai Hu[1] · Tianjun Zhou[1,2] · Dongdong Peng[3] · Wanyi Jiang[1,2] · Bo Lu[4] · Bo Wu[1] · Xiaolong Chen[1] · Lixia Zhang[1] · Wenxia Zhang[1]

Received: 20 November 2023 / Accepted: 7 February 2024

Abstract
The Yangtze River Valley (YRV) experienced an unprecedented heatwave in midsummer of 2022. Still, the detailed physical processes involved in the influence of abnormal large-scale atmospheric circulation on the heatwave remain unexplored. Here, we show that the positive meridional gradient of anomalous atmospheric moisture at the middle-lower troposphere and associated extreme dry air advection over the YRV are vital prerequisites for forming the 2022 YRV heatwave. The 2022 YRV heatwave is dominated by interannual variability, contributing 72.7% to the total temperature anomalies. Diagnosis of the surface heat budget equation indicates that the surface cloud radiative forcing is the most critical process in driving the 2022 YRV heatwave, which is dominated by the positive surface short-wave cloud radiative forcing associated with the suppressed precipitation and the middle-low clouds. The suppressed precipitation is induced by the vertical dynamical processes of anomalous moisture advection caused by the abnormal descending flows over the YRV, which are driven by the negative advection of anomalous latent heat energy by climatological meridional wind (anomalous dry air advection) according to the atmospheric moist static energy equation. Simulations from the Lagrangian model FLEXPART further indicate that the moisture anomaly over the north of YRV mainly originated from the surface evaporation in the YRV, implying that there is a positive land-air feedback during the life cycle of the YRV heatwave. Our study enriches the mechanism understanding of the 2022 YRV heatwave from the perspective of surface energy budget and land-air feedback.

1 Introduction

During the boreal midsummer (July–August) of 2022, the Yangtze River Valley (YRV) experienced an unprecedented intense, and prolonged heatwave, with the maximum temperature exceeding 40 °C (Mallapaty 2022; Lu et al. 2023). A worst hydrologic drought followed the extreme YRV heatwave (Ma et al. 2022). Eventually, it led to a severe compound extreme, significantly impacting human health, agriculture, water and energy supplies (Yuan et al. 2023). The severity of the 2022 YRV extreme heatwave highlights the importance of unravelling the underlying mechanisms to serve accurate climate prediction and adaptation planning.

Abnormal large-scale atmospheric circulation background and its associated lower boundary conditions are the essential prerequisites for the occurrence and maintenance of extreme climate events (Wang et al. 2014; Choi et al. 2020; Ha et al. 2022), and several efforts have been devoted to understanding the formation process of the large-scale circulation background associated with the 2022 YRV heat event (Zhang et al. 2023; Wang et al. 2023; Tang et al. 2023). It is generally acknowledged that the merged subtropical high belt over the Asian continent is critical to the 2022 YRV heat event, which is a consequence of the synergistic effects of the westward extension of the low-level western North Pacific subtropical high (WNPSH) and the eastward extension of the upper-level South Asian high (SAH) (Chen and Li 2023). The merge of the two subtropical high systems formed initially in July and intensified in August (Zhang

✉ Tianjun Zhou
zhoutj@lasg.iap.ac.cn

[1] State Key Laboratory of Numerical Modeling for Atmospheric Sciences and Geophysical Fluid Dynamics, Institute of Atmospheric Physics, Chinese Academy of Sciences, Beijing, China

[2] College of Earth and Planetary Sciences, University of Chinese Academy of Sciences, Beijing, China

[3] Institute of Tropical and Marine Meteorology, China Meteorological Administration, Guangzhou, China

[4] National Climate Center, China Meteorological Administration, Beijing, China

Published online: 25 March 2024

et al. 2023). In July of 2022, the extraordinary circulation anomalies are suggested to be driven by the diabatic heating associated with the flooding in Pakistan (Wang et al. 2023), the La Niña SSTA pattern (Tang et al. 2023), the enhanced convection over the tropical eastern Indian Ocean (Chen and Li 2023), and the atmospheric intraseasonal oscillation (Liu et al. 2023). While in August, the negative phase of the Silk Road pattern (SRP) (Lu et al. 2002; Enomoto et al. 2003; Ding and Wang 2005) cooperates with the above processes to intensify the circulation anomalies (Zhang et al. 2023; Wang et al. 2023). In addition, the role of local land–air feedback caused by the dry soil moisture in the 2022 YRV heatwave was also emphasised (Jiang et al. 2023), which can amplify the heatwave by reducing the evapotranspiration and increasing the upward sensible flux (Erdenebat and Sato 2018; Thompson et al. 2022), or internal land-atmosphere interactions (Seo et al. 2020).

The existing studies commonly assumed that the heatwave was driven by large-scale anomalous anticyclonic circulation via adiabatic heating from descending flows and enhancement of incoming solar radiation. However, the detailed physical processes remain unexplored. What is the relationship between the large-scale circulations and the extreme 2022 YRV heat wave? What are the detailed physical processes underlying the formation of the extreme 2022 YRV heat wave? This study aims to answer these two questions via rigorous diagnostic analysis. The following sections of the paper will be outlined for clarity. Section 2 introduces observational datasets and analytical methods. Section 3 investigates the detailed physical processes responsible for the 2022 YRV heatwave. The concluding remarks and discussions are given in Sect. 4.

2 Data and methods

2.1 Observations

In this study, we used the monthly surface air temperature (SAT), surface radiations and heat fluxes, cloud cover, atmospheric circulations, precipitation, and evaporation data from the fifth-generation European Centre for Medium-Range Weather Forecasts reanalysis (ERA5) (Hersbach et al. 2020) for the period 1960–2022 and the National Centers for Environmental Prediction (NCEP) Climate Forecast System Reanalysis (CFSR) (Saha et al. 2010, 2014) for the period 1979–2022. Note that the CFSR datasets include the CFSR V1 (from 1979 to 2010) and V2 (from 2011 to 2022). The ERA5 atmospheric dataset has a high horizontal resolution of 0.25°×0.25°, with 37 pressure levels from 1000 hPa to 1 hPa. The CFSR global atmosphere resolution is ~38 km (T382) with 64 levels extending from the surface to 0.26 hPa. Both ERA5 and CFSR can accurately reproduce the 2022 YRV heatwave (Li et al. 2023; He et al. 2023).

2.2 Analytical method

To investigate the physical processes responsible for the 2022 YRV heatwave, we diagnose the linearised surface heat budget equation (Lu and Cai 2009), which can be written as:

$$\begin{aligned}\Delta T \approx \frac{1}{4\sigma \bar{T}_s^3}\Delta F^{\uparrow} = \frac{1}{4\sigma \bar{T}_s^3}[-(\Delta\alpha)\left(\bar{S}^{\downarrow} + \Delta S^{\downarrow}\right) \\ + \Delta CRF_s + \left(1-\bar{\alpha}\right)\Delta S^{\downarrow,clr} + \Delta F^{\downarrow,clr} \\ - \Delta Q - \Delta(H+LE)]\end{aligned} \tag{1}$$

where T is the surface temperature.$F^{\downarrow}$ and $F^{\uparrow}$ are surface downward and upward long-wave (LW) radiations with $F^{\uparrow} \approx \sigma T_s^4$ according to Stefan-Boltzmann law. $S^{\downarrow}$ and $S^{\uparrow}$ are surface downward and upward short-wave radiations. α is the surface albedo, which can be derived from the ratio of of $S^{\uparrow}$ to $S^{\downarrow}$ at surface. $(\bullet)^{clr}$ represents the surface clear-sky radiations. H and LE are surface sensible and latent heat fluxes. Q is the heat storage term. The overbar denotes the unperturbed mean climate state, and the Δ represents the perturbation relative to the mean climate state. The terms on the righthand side of Eq. (1) represent six different processes with effect on temperature change, including the surface albedo feedback (SAF), the change in surface cloud radiative forcing (ΔCRF_s), the non-SAF-induced change in clear-sky shortwave radiation, the change in downward clear-sky longwave radiation fluxes, the change in heat storage, and the changes in surface sensible/latent fluxes, respectively.

The ΔCRF_s with the SAF excluded can be decomposed into two terms as:

$$\Delta CRF_s = \left(1-\bar{\alpha}\right)\Delta S^{\downarrow,cld} + \Delta F^{\downarrow,cld} \tag{2}$$

where $(\bullet)^{cld}$ is the difference between the surface total-sky radiation and the surface clear-sky radiation, which represents the cloud radiative forcing. $\bar{\alpha}$ is the surface albedo of the unperturbed mean climate state.

To comprehend the physical mechanisms that determine the changes in YRV's midsummer rainfall, following Chou et al. (2013) and Hu et al. (2021), the atmospheric moisture flux equation, integrated over a column and linearized, was diagnosed in the following manner:

$$\begin{aligned}P' = E' - <\bar{V}\bullet\nabla_h q'> - <\bar{\omega}\bullet\partial_p q'> \\ - <V'\bullet\nabla_h \bar{q}> - <\omega'\bullet\partial_p \bar{q}> + NL + Residual\end{aligned} \tag{3}$$

where q is specific humidity, $\boldsymbol{V}$ is horizontal wind, ω is vertical pressure velocity, P is precipitation, E is surface evaporation, and the angle bracket <> denotes the mass-weighted vertical integral through the entire atmospheric column. h and p represent the horizontal and vertical dimensions The NL is the nonlinear component, and the $Residual$ denotes the residual term. The overbars (primes) represent the climatological monthly mean (the monthly anomaly).

To investigate the mechanisms responsible for the anomalous vertical motion, the linearised column-integrated moist static energy (MSE) equation (Neelin and Held 1987; Wu et al. 2017) was diagnosed as follows:

$$< \omega' \partial_p \bar{h} > \approx F'_{net} - < u' \partial_x \left(C_p T + L_v q\right) > - <\bar{u}\, \partial_x \left(C_p T + L_v q\right)' > - < v' \partial_y \left(C_p T + L_v q\right) >$$

$$- <\bar{v}\, \partial_y \left(C_p T + L_v q\right)' > - <\bar{\omega}\, \partial_p h' > + NL \quad (4)$$

where F_{net} represents the net flux into the atmospheric column. The h denotes the MSE, which can be written as $h = C_P T + L_v q + \varphi$. The $(C_p T + L_v q)$ is the moist enthalpy. C_P and L_v are the specific heat at constant pressure and the latent heat of vaporization, respectively; T denotes the air temperature; q is the specific humidity; φ denotes the geopotential; u, v and ω represent the zonal wind, meridional wind and vertical velocity, respectively; x, y and p represent the zonal, meridional and vertical direction, respectively. The negative terms on the righthand side of Eq. (4) can drive anomalous descending motion under the constraints of the MSE budget balance (Biasutti et al. 2018).

The atmospheric precipitable water vapour (PW) and the vertically integrated moisture flux (Q) (Zhou and Yu 2005) were calculated as

$$PW = \frac{1}{g} \int_{100}^{p_s} q dp \quad (5)$$

$$Q = \frac{1}{g} \int_{100}^{p_s} q \boldsymbol{V} dp \quad (6)$$

where q is specific humidity; $\boldsymbol{V}$ is horizontal wind vector; p is pressure, p_s is surface pressure, and g is the acceleration due to gravity.

The monthly anomalies were obtained by removing the mean monthly climatology of 1991–2020. The interannual variability is estimated by the difference between the original anomalies and the 9-year moving average. The long-term linear trend is calculated by the linear trend of the 9-year moving average, and the difference between the 9-year moving average and the long-term linear trend represents the interdecadal variability.

2.3 FLEXPART simulations

To identify the geographical moisture source regions of the anomalous atmospheric moisture accumulations over the region to the north of YRV in midsummer of 2022, we employed the Lagrangian model FLEXPART v9.2. The FLEXPART model was developed by the Norwegian Institute for Air Research, which can be used to accurately describe the moisture-transporting processes associated with atmospheric circulations by analysing the trajectories of corresponding air particles (Stohl et al. 2005). In this study, the FLEXPART simulations were conducted forward in time with the "domain fill" option for the midsummer during 1979–2022 based on the 6-hourly CFSR dataset. The setting options of conducted FLEXPART simulations are referred to Peng et al. (2020, 2022), with a total of one billion particles released over the globe region to split the global atmosphere into the corresponding air particles with equal mass. The outputs of FLEXPART simulations are the information of the one billion air particles, which include the identity number, three-dimensional positions (above ground level, latitude, longitude) and meteorological variables (the humidity, air mass, temperature, and so on). The time intervals of outputs are 6 h. To explore the moisture sources of the atmosphere in this study, all the air particles over the study region are tracked backwards for 10 days (the mean residual time of atmospheric vapour) by employing the moisture source attribution method (Sodemann et al. 2008). The official website of the FLEXPART model is https://www.flexpart.eu/.

3 Results

3.1 The 2022 YRV heatwave and its associated circulation anomalies

The maximal surface warmings associated with the 2022 midsummer YRV heatwave exhibit a zonally elongated structure, spanning from the northern Tibetan Plateau to the entire YRV (Fig. 1a). The area-averaged SAT anomalies over the YRV in midsummer of 2022 relative to the 1991–2020 climatology is 1.98 °C, which sets the highest record for the period 1960–2022 (Fig. 1b). The SAT anomalies over the YRV in 2022 involve signals with different timescale, including the long-term linear trend, the interdecadal variability, and the interannual variability. Estimations of their

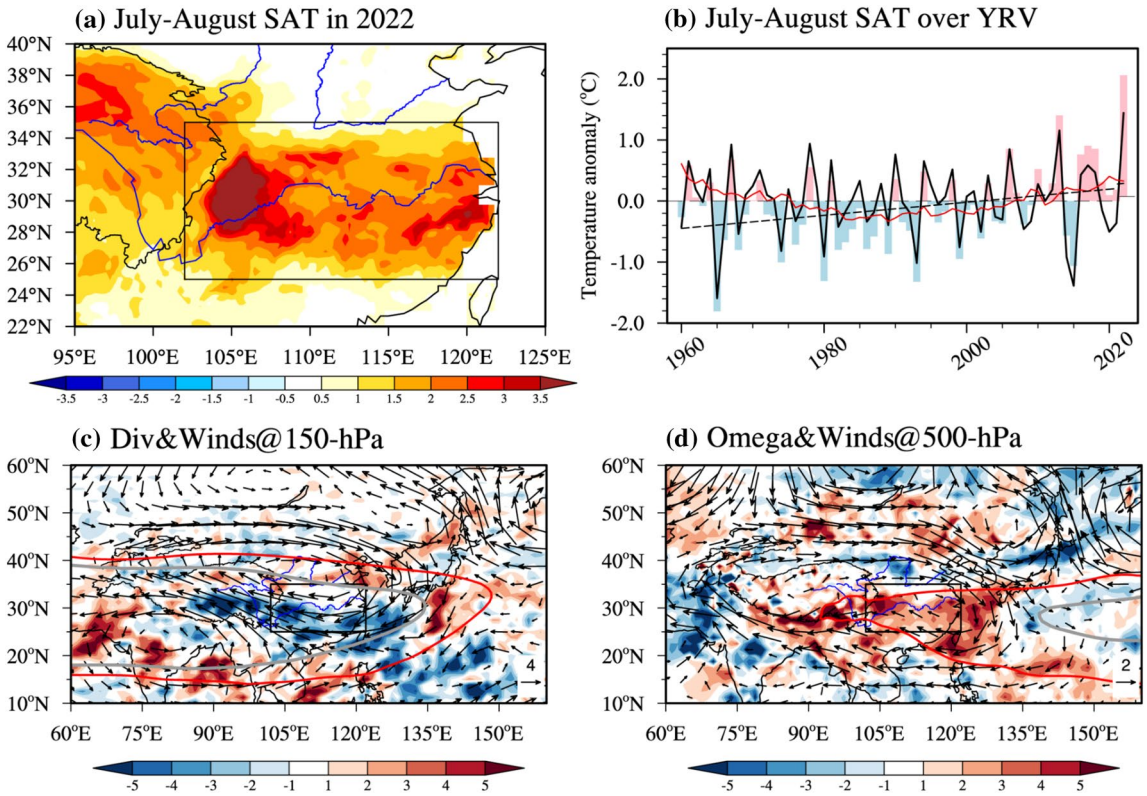

Fig. 1 The 2022 midsummer (June–July) heatwave in the Yangtze River Valley (YRV) and its associated circulation anomalies. **a** July-August mean surface air temperature (SAT) anomalies in 2022, unit: °C. The SAT anomalies are relative to the period of 1991–2020. **b** Time series of the July-August mean SAT anomalies averaged over the YRV from 1960 to 2022. The original SAT anomalies, and the components of linear trend, interdecadal variability, and interannual variability are represented by a bar, dashed black line, red line, and solid black line, respectively. **c** July-August mean atmospheric divergence (shading, unit: 10^{-6} s^{-1}) and horizontal winds (vector, unit: $m{\cdot}s^{-1}$) anomalies at 150-hPa. **d** July-August mean vertical pressure velocity (shading, unit: $Pa{\cdot}s^{-1}$) and horizontal winds (vector, unit: $m{\cdot}s^{-1}$) anomalies at 500-hPa. In **c**, **d**, the July-August mean edges of the South Asian high (SAH) at 150-hPa, and the Western Pacific subtropical high (WPSH) at 500-hPa are denoted by the 14,300 gpm and 5880 gpm contour of geopotential height, respectively, where the (red) grey line represents the case in 2022 (the climatology for 1991–2020). The black boxes in (**a**, **c**, **d**) denote the YRV (25°–35°N,102°–122°E). The results were obtained from ERA5.

relative contribution show that the 2022 YRV heatwave is dominated by the component of interannual variability, which contributes 1.44 °C to the total temperature anomalies in midsummer of 2022, accounting for 72.7% of the anomaly amplitude.

The circulation anomalies associated with the extreme heatwave in midsummer 2022 are the eastward shift of the SAH in the upper troposphere (Fig. 1c) and the westward extension of the WNPSH in the middle-lower troposphere (Fig. 1d). Although the border of the SAH in midsummer of 2022 lies within the range of historical variations for the period 1960–2022, the westward extension of the WNPSH in the 500-hPa level breaks the record held since the year 1960 (Fig. S1). The overlaps of the two subtropical high systems produce an anomalous anticyclone in the middle to upper troposphere over the YRV, accompanied by atmospheric divergence and descending motion along the southern edge of the anomalous anticyclone. It is generally acknowledged that high-pressure circulation systems can induce descending motion and favour the occurrence of heat waves. The westward shift of the WNPSH covers the whole YRV and a large part of the Western North Pacific, while the anomalous descending motions only occur at the upper and lower reaches of YRV and the adjacent sea (Fig. 1d). How does the anomalous descending motions over the YRV come into existence in midsummer of 2022? What are the detailed mechanisms underlying the influence of the anomalous descending motions on the extreme YRV heatwave? We will address these questions in the following analyses.

3.2 Budget analysis for the 2022 YRV heatwave

To quantitatively evaluate the contributions of different processes to the 2022 YRV heatwave, the surface heat budget

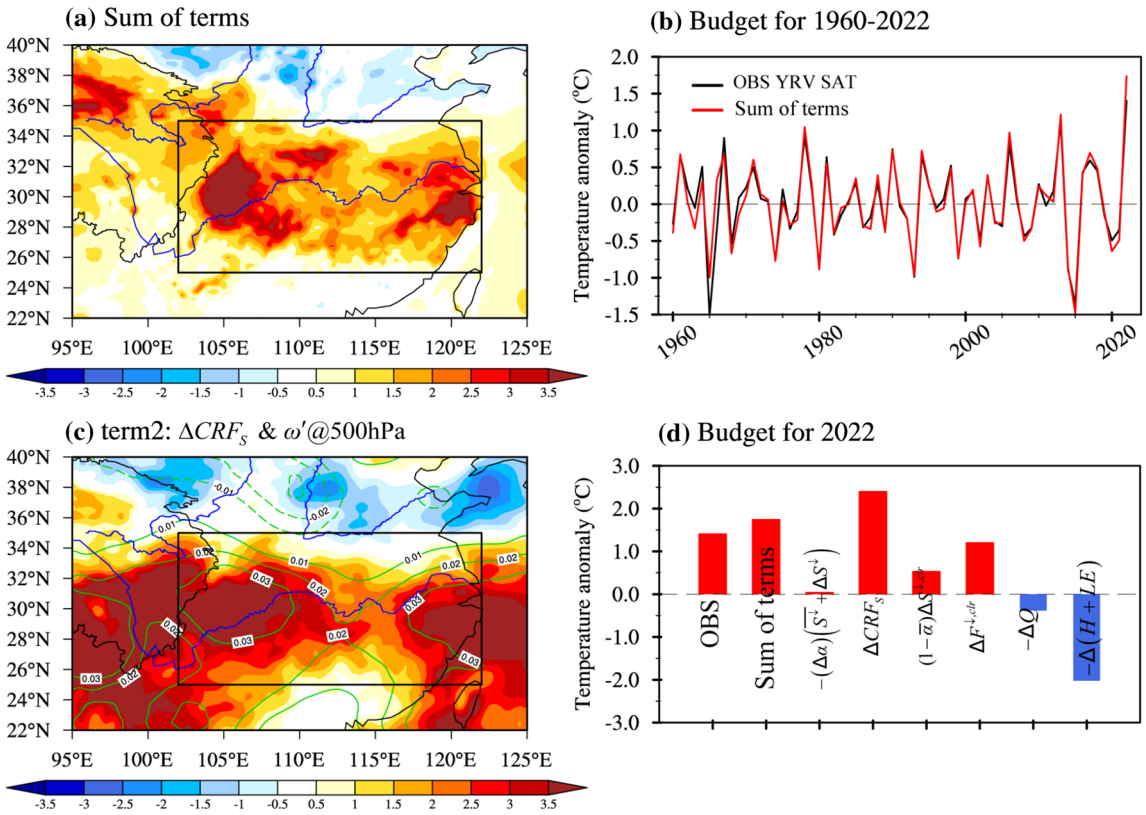

Fig. 2 Budget analysis of the surface heat budget equation [Eq. (1)] for the 2022 midsummer heat wave in the YRV. **a** the sum of the six terms on the right-hand side of Eq. (1). Unit: °C. **b** budget for the interannual variability of the July-August mean YRV SAT anomalies for 1960–2022. The red (black) line represents the sum of the six budget terms (observed YRV SAT), respectively. **c** the SAT anomalies contributed by the change in surface cloud radiative forcing (ΔCRF_s) (shading, unit: °C), and vertical velocity anomaly at 500-hPa (contour, unit: Pa·s^{-1}, the interval is 0.01; the positive (negative) values are shown in solid (dashed) lines; zero contour is not shown). **d** the partial changes from six individual feedback processes to the positive surface temperature anomalies associated with the 2022 YRV heatwave. From left to right in the abscissa: the SAT anomalies averaged over the YRV for the observation (OBS), the sum of the six terms, and contributions from the surface albedo feedback, the change in ΔCRF_s, the non-SAF-induced change in clear-sky short-wave radiation, the change in downward clear-sky longwave radiation fluxes, the change in heat storage, and the changes in surface sensible/latent fluxes, respectively. Unit: °C. The black boxes in **a**, **c** denote the YRV (25°–35°N,102°–122°E). The results were obtained from ERA5.

equation [Eq. (1)] was diagnosed on the interannual time scale. The sum of the six terms on the right-hand side of Eq. (1) reasonably reproduces the 2022 YRV heatwave, with the area-averaged surface temperature anomalies over the YRV resulting from six feedback processes reaching 1.74 °C (Fig. 2a). The budgets also can reproduce the interannual variability of the midsummer SAT anomalies for the period 1960–2022, with the correlation coefficient reaching 0.96 (Fig. 2b). These results suggest that the budget of surface heat budget equation are reliable in term of representing the midsummer SAT variations over the YRV.

The partial changes from individual feedback processes to the positive surface temperature anomalies associated with the 2022 YRV heatwave are quantitatively estimated in Fig. 2d. Among these processes, the surface cloud radiative forcing (ΔCRF_s) is the most critical process, which contributes 2.39 °C to the total anomalies. The term surface turbulent fluxes ($-\Delta(H + LE)$) has a cooling effect (− 2.02 °C) to the surface warming, which represents the enhanced evapotranspiration and upward sensible flux due to the surface warmings, and in turn, acts to reduce the surface warmings. To understand the driving processes of the 2022 YRV heatwave, we need to focus on the positive ΔCRF_s. The ΔCRF_s can be further decomposed into two terms, the surface short-wave CRF and the surface long-wave CRF according to Eq. (2). As shown in Fig. 3, the ΔCRF_s is dominated by the surface short-wave CRF (Fig. 3a, b), which spatial distributions resemble the anomalies of precipitation and middle and low clouds (Fig. 3c, d). When the precipitation is suppressed, the associated decreased middle and low clouds lead to increased surface incoming short-wave radiations, further driving the surface warmings. So, the next question is why the precipitation over the YRV was suppressed in midsummer of 2022.

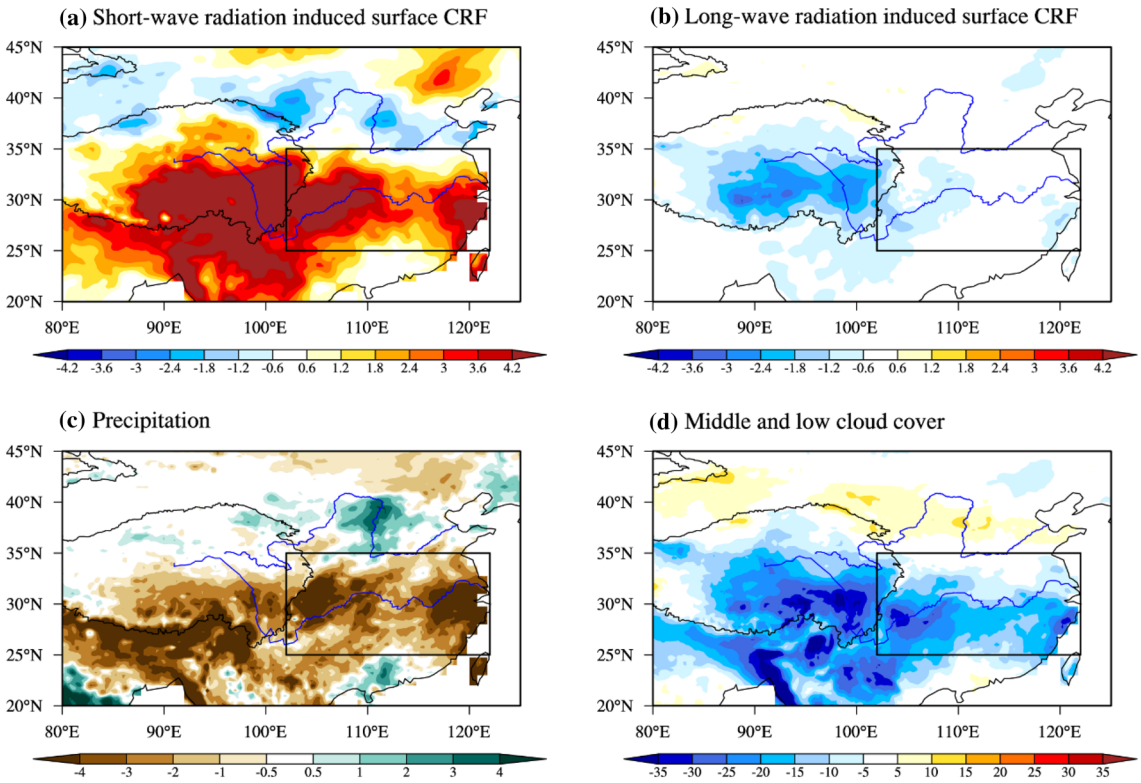

Fig. 3 Formation processes of the surface cloud radiative forcing in midsummer of 2022. **a**, **b** the July–August mean surface cloud radiative forcing induced by the surface short-wave radiation (**a**), and the surface long-wave radiation (**b**), unit: °C. **c**, **d** the July–August mean precipitation (unit: mm·day^{-1}) (**d**), and the middle and low cloud cover (unit: %). The results were obtained from ERA5.

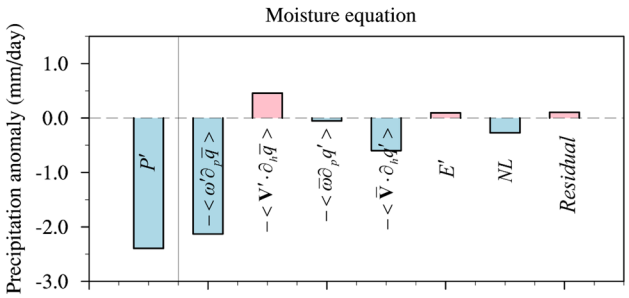

Fig. 4 Budget analysis for the moisture equation [Eq. (3), units: mm·day^{-1}] for the 2022 midsummer in the YRV (25°–35°N,102°–122°E). The results were obtained from ERA5.

According to the atmospheric moisture budget analysis, the negative precipitation anomalies are dominated by the vertical dynamical processes of anomalous moisture advection ($-<\omega' \bullet \partial_p q>$) (Figs. 4 and 5). Quantitatively, the precipitation anomalies averaged over the YRV is − 2.32 mm/day, with the contribution from $-<\omega' \bullet \partial_p q>$ reaching − 2.12 mm/day, accounting for 91% of the precipitation variations. The $-<\omega' \bullet \partial_p q>$ is linked dynamically with the anomalous vertical velocity, and the descending motion at 500 hPa over the YRV well coincides with the $-<\omega' \bullet \partial_p \bar{q}>$ (Fig. 5a). Hence, the spatial pattern of the ΔCRF_s is also in accord with the descending motion at 500 hPa, which isoline of 0.03 Pa·s−1 well coincides with the maximum values of ΔCRF_s and SAT anomalies (Fig. 2c). The interannual variations of midsummer SAT anomalies in the YRV during 1960–2022 is also closely related with the area-averaged anomalous vertical velocity at 500 hPa over the YRV, with the correlation coefficient reaching 0.59 ($p < 0.01$) (not shown). The results suggest that the anomalous descending motion is associated with the YRV heatwave through the surface short-wave CRF, which is dynamically linked with the changes in precipitation and cloud cover.

In midsummer of 2022, the anomalous descending motion at 500 hPa over the YRV at interannual timescales is the strongest since 1960 (Fig. 6b). What are the formation processes of the anomalous vertical motions? We further diagnosed the MSE equation [Eq. (4)] to the regions with the 500 hPa vertical velocity anomalies above 0.03 Pa·s^{-1} in YRV. The column-integrated MSE equation can accurately represent the 500 hPa vertical velocity anomalies above these regions for the period of 1960–2022 (Fig. 6b). For the midsummer of 2022, the budget results

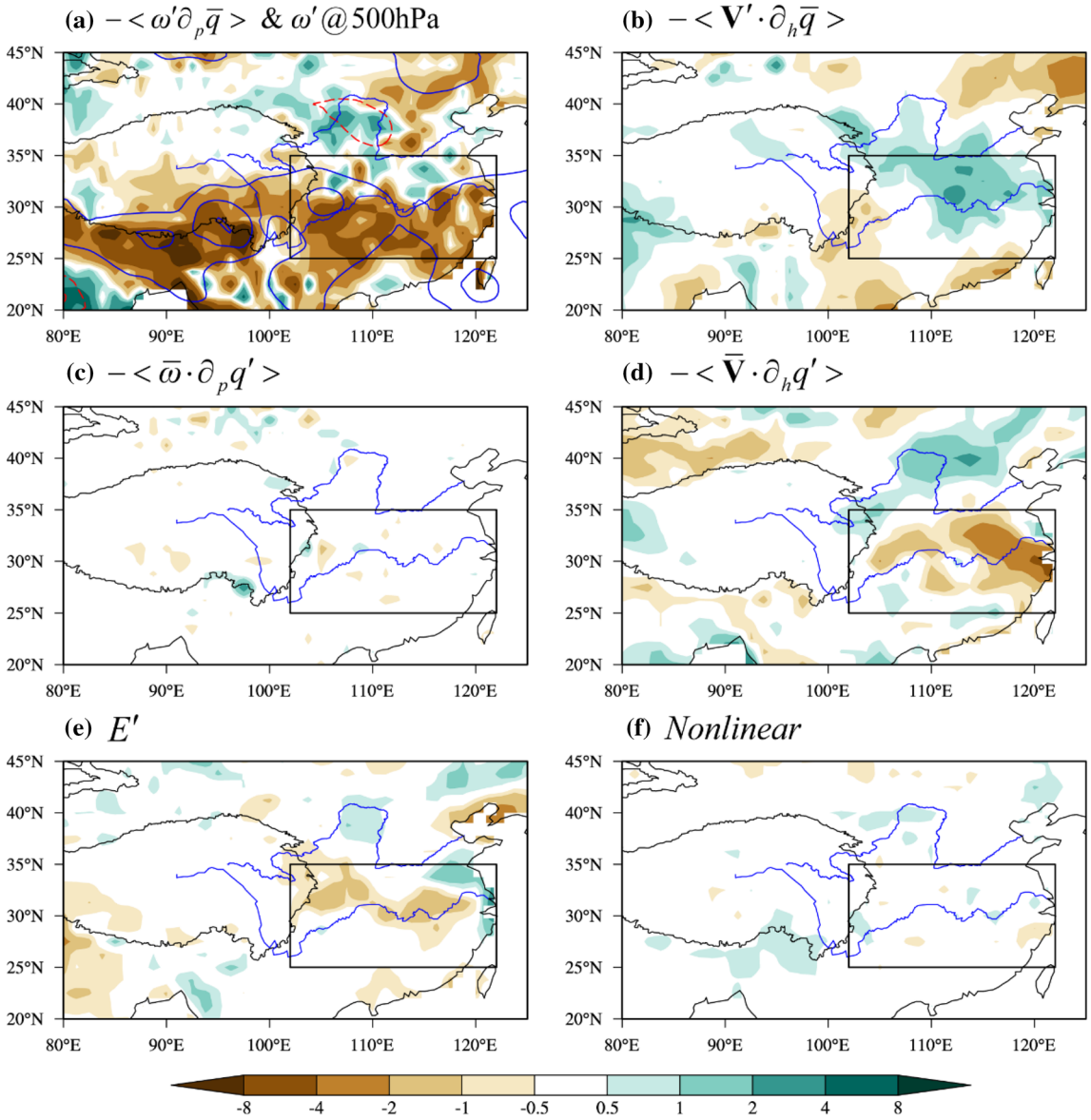

Fig. 5 Budget analysis of the column-integrated atmospheric moisture flux equation [Eq. (3)] for the 2022 midsummer in the YRV. **a** the vertical dynamic component of the vertically integrated moisture advection term ($-<\omega'\partial_p\bar{q}>$, shading) and the anomalous vertical pressure velocity at the 500 hPa (contour, the interval is 0.02; the positive (negative) values are shown in solid (dashed) lines; zero contour is not shown). **b** the horizontal dynamic component of the vertically integrated moisture advection term ($-<\boldsymbol{V}'\bullet\nabla_h\bar{q}>$). **c** the vertical thermodynamic component of the vertically integrated moisture advection terms ($-<\bar{\omega}\bullet\partial_p q'>$), **d** the horizontal thermodynamic component of the vertically integrated moisture advection terms ($-<\boldsymbol{V}\bullet\nabla_h q'>$), **e** the surface evaporation term ($E\prime$), and **f** the nonlinear components (NL). The units of the vertically integrated moisture advection term and anomalous vertical pressure velocity are mm·day^{-1} and Pa·s^{-1}. The black boxes denote the YRV (25°–35°N,102°–122°E). The results were obtained from ERA5.

suggest that the anomalous descending motions were driven by the anomalous negative advection of anomalous moist enthalpy by climatological meridional wind ($-<\bar{v}\,\partial_y\left(C_pT+L_vq\right)'>$), and the anomalous meridional dry air advection ($-<\bar{v}\,\partial_y\left(L_vq\right)'>$) has the most prominent contributions (Fig. 6a). The $-<\bar{v}\,\partial_y\left(L_vq\right)'>$ in 2022 is also the strongest since 1960, consistent with the extreme anomalous descending motions (Fig. 6b).

The $-<\bar{v}\,\partial_y\left(L_vq\right)'>$ in 2022 has negative value centres over the YRV (Fig. 6c), and this negative moist enthalpy advection decreases the atmospheric moist static energy and facilitate suppressed local convection under the constraints of the MSE budget balance. From the longitude–height cross

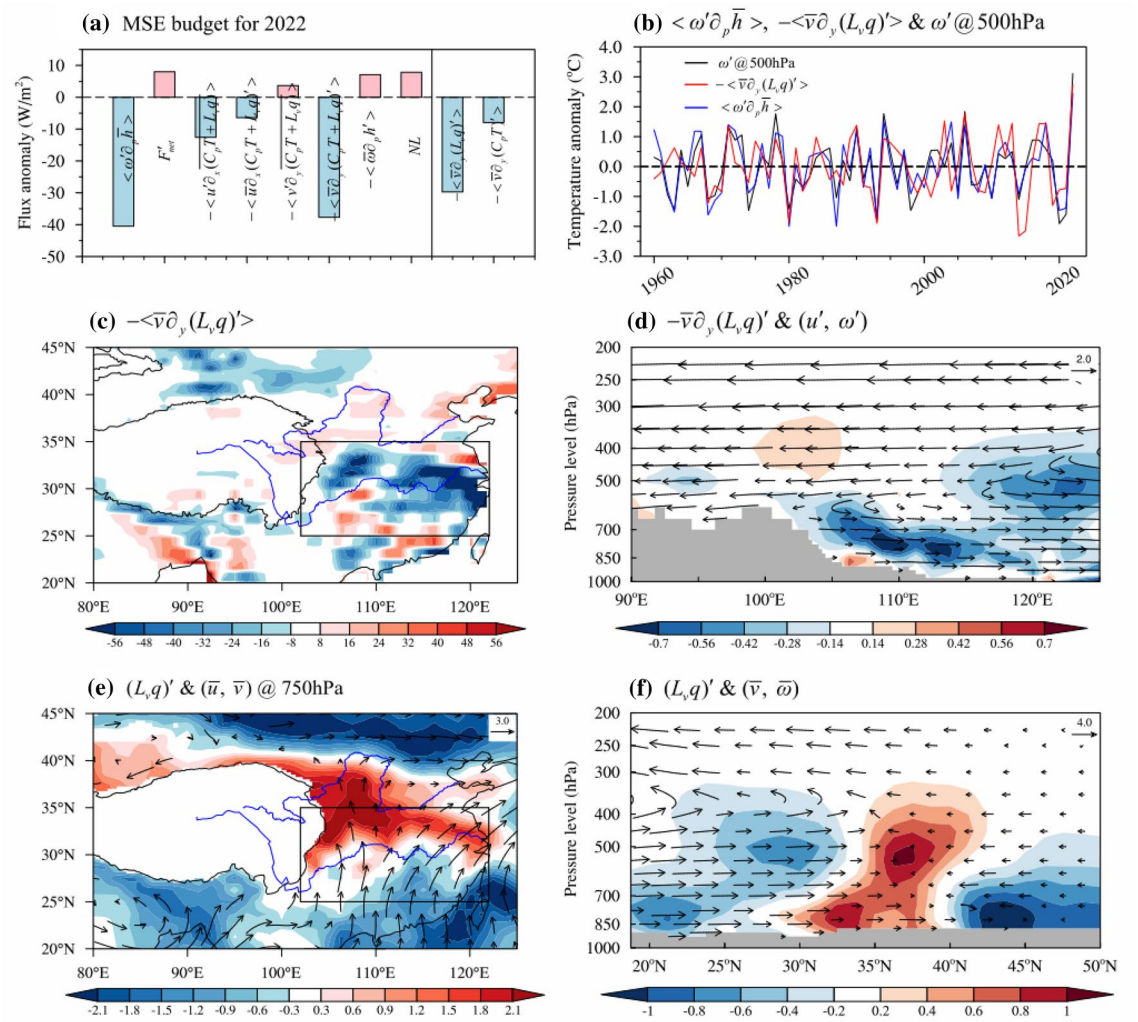

Fig. 6 Budget analysis of column-integrated moist static energy (MSE) equation [Eq. (4)] for the anomalous vertical velocity over the YRV. **a** Each budget term of the MSE equation for the anomalous vertical velocity over the YRV in midsummer of 2022. Unit: $W{\cdot}m^{-2}$. The budget is conducted to the regions within the YRV with 500 hPa vertical velocity anomalies above 0.03 $Pa{\cdot}s^{-1}$. **b** The anomalous vertical velocity at 500 hPa (black line), the vertically integrated anomalous vertical advection of climatological mean MSE ($<\omega'\partial_p h>$, red line), and the vertically integrated anomalous meridional advection of anomalous latent heat energy by climatological wind ($-<\bar{v}\,\partial_y(L_vq)'>$, blue line) averaged over the regions of MSE budget for the period 1960–2022. The time series are standardised. **c** the spatial pattern of $-<\bar{v}\,\partial_y(L_vq)'>$ in the midsummer of 2022, unit: $W{\cdot}m^{-2}$. **d** The longitude–height cross section of $-\bar{v}\,\partial_y(L_vq)'$ (unit: $10^{-3}\ J{\cdot}kg^{-1}{\cdot}s^{-1}$) and anomalous zonal and vertical winds (unit: $m{\cdot}s^{-1}$) along 25°–35°N. **e** The spatial pattern of anomalous latent heat energy (unit: $10^3\ J{\cdot}kg^{-1}$) and climatological horizontal winds at 750-hPa (unit: $m{\cdot}s^{-1}$). **f** The latitude–height cross-section of the anomalous latent heat energy (shading, unit: $2\times10^3\ J{\cdot}kg^{-1}$) and the climatological meridional and vertical winds (vector, unit: $m{\cdot}s^{-1}$) along 102°–122°E. The black boxes in (**c** and **e**) denote the YRV (25°–35°N, 102°–122°E). The results were obtained from ERA5.

section averaged over the YRV, the maximum anomalies of $-\bar{v}\,\partial_y(L_vq)'$ emerge at the levels between 850 and 700 hPa over the YRV, directly corresponded with the anomalous descending motions at these levels (Fig. 6d). We utilized the 750 hPa level to investigate the formation of $-<\bar{v}\,\partial_y(L_vq)'>$. It can be found that there are positive latent heat energy anomalies over the region between the Yangtze and Yellow Rivers, and negative latent heat energy anomalies over the northern South China Sea, which result in a positive meridional gradient of anomalous latent heat energy ($\partial_y(L_vq)'$) over the YRV (Fig. 6e). Under the background of the climatological East Asian summer monsoon circulations, the negative $-\bar{v}\,\partial_y(L_vq)'$ is thus generated. The latitude–height cross section of latent heat energy anomalies also indicates that the positive $\partial_y(L_vq)'$ is mainly determined by the meridional gradient of anomalous atmospheric moisture at the middle-lower troposphere (Fig. 6f), and the atmospheric moisture accumulation to the north of YRV plays an important role. Hence, it is vital to investigate the abnormal atmospheric moisture

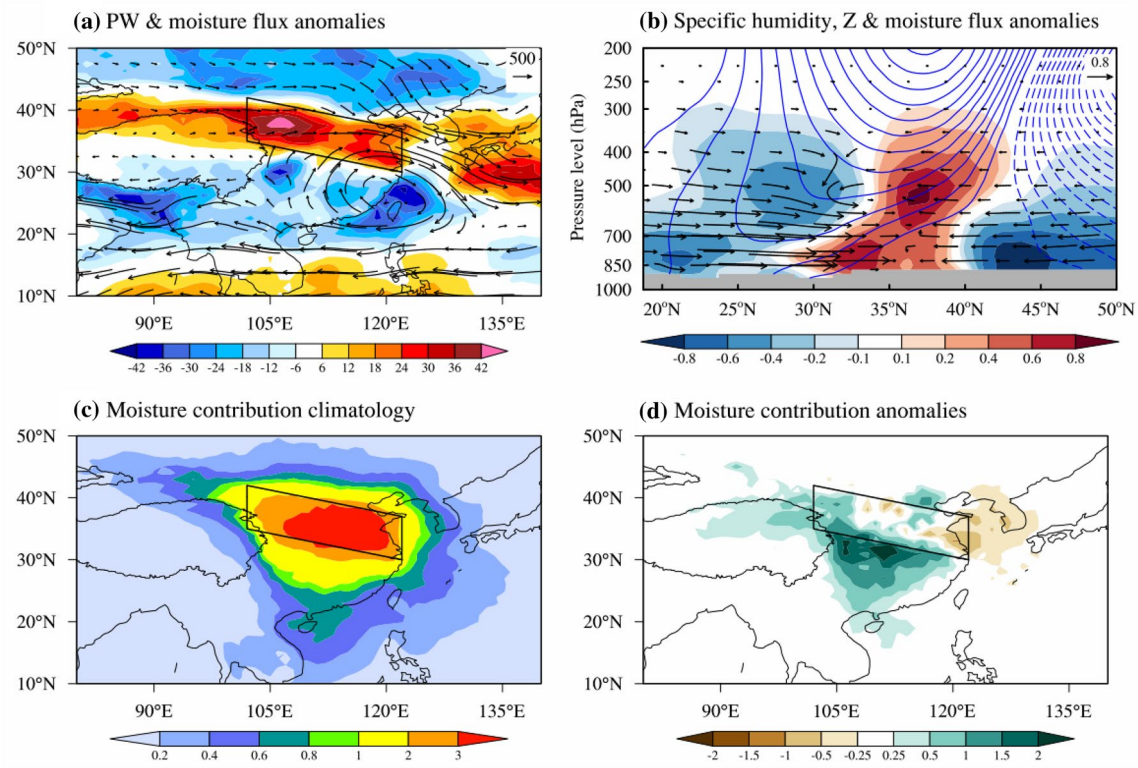

Fig. 7 The anomalous atmospheric moisture transportations in midsummer of 2022. **a** the atmospheric precipitable water vapor (PW; shading, unit: $kg{\cdot}m^{-2}$) and the vertically integrated moisture flux (Q; vector, unit: $kg{\cdot}m{\cdot}s^{-1}$) anomalies in midsummer of 2022. **b** the latitude–height cross-section of the moisture flux (vector, unit: $g{\cdot}m{\cdot}s^{-1}{\cdot}kg^{-1}$), specific humidity (shading, unit: $g{\cdot}kg^{-1}$), and geopotential (contour, unit: $m^2{\cdot}s^{-2}$) anomalies in midsummer of 2022 averaged along 102°–122°E. **c** the moisture contribution associated with climatological mean midsummer atmospheric water contents for the region north of YRV (black box) derived from all the target back-tracking trajectories over days 10–1 in the FLEXPART simulations. Unit: 10^{11} kg. **d** as in **c**, but for the moisture contribution anomalies associated with the midsummer of 2022. The results in **a**, **b** were obtained from ERA5, and the FLEXPART simulations in **c**, **d** were based on the CFSR

transportation in midsummer of 2022 to understand the formation of the extreme meridional dry air advection.

3.3 Abnormal moisture transportation in midsummer of 2022

The atmospheric precipitable water vapour and the vertically integrated moisture flux anomalies in midsummer of 2022 are shown in Fig. 7a. The most prominent feature is that the atmospheric moisture unusually accumulates to the north of YRV, with less moisture on both the north and south sides. The anomalous moisture accumulations are closely associated with the anticyclonic moisture flux anomalies above South China and the southward moisture flux anomalies above North China (Fig. 8), implying the critical role of large-scale circulations. The vertical profiles of moisture to the north of YRV distribute along the high-pressure ridge line (Fig. 8), which indicates that the merge of the SAH and WNPSH over the YRV plays an essential role in anomalous moisture transportations. According to previous study, the merge of the SAH and WNPSH in midsummer of 2022 could be driven by the diabatic heating associated with the flooding in Pakistan (Wang et al. 2023), the La Niña SSTA pattern (Tang et al. 2023), the enhanced convection over the tropical eastern Indian Ocean (Chen and Li 2023), the atmospheric intraseasonal oscillation (Liu et al. 2023), and the negative phase of the SRP (Wang et al. 2023).

The moisture contribution associated with climatological mean midsummer atmospheric water contents for the region to the north of YRV (black box in Fig. 7a) over the whole 10-day back-tracking period derived from the FLEXPART simulations are shown in Fig. 7c. The highest centre of moisture contribution occurs at the north of YRV, implying that the local evaporation is the main contributor to the atmospheric moisture over the north of YRV (Fig. 7c). Concerning the climate mean, the distributions of moisture contribution anomaly of the midsummer in 2022 show that there are increments in moisture contribution over the middle and upper reaches of the YRV but decrements in moisture

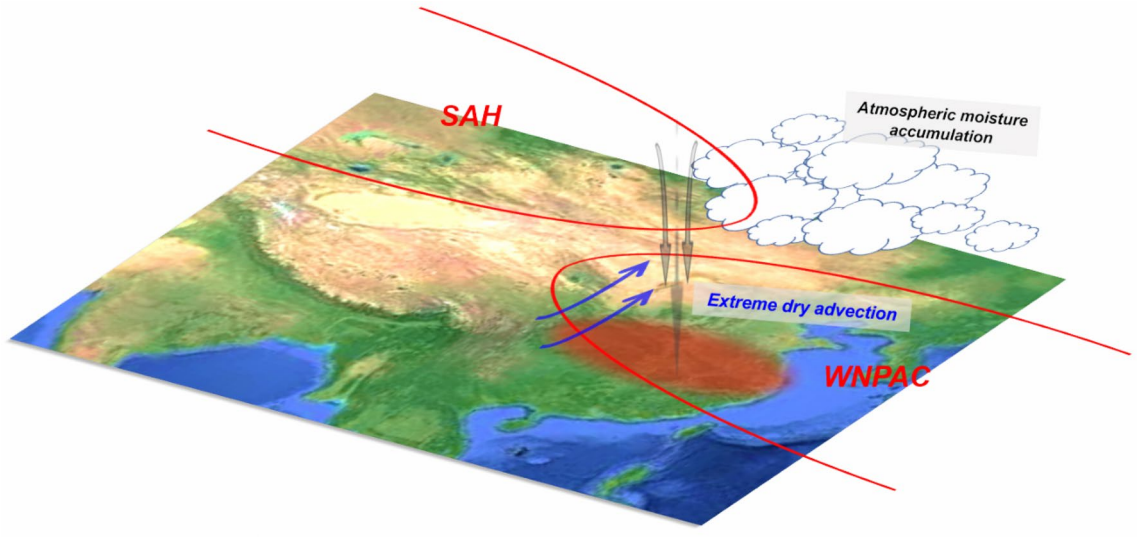

Fig. 8 Schematic of the influence of extreme dry advection on the record-breaking Yangtze River heatwave in midsummer of 2022. The 2022 YRV heatwave is driven by the positive surface short-wave cloud radiative forcing, induced by the extreme negative advection of anomalous latent heat energy by climatological meridional wind (anomalous dry air advection). The anomalous dry air advection is linked dynamically with the moisture accumulations over the north of YRV, which are originated from the surface evaporation in the YRV during the heatwave

contribution over the Yellow Sea (Fig. 7d), which indicate that the atmospheric moisture anomaly over the north of YRV mainly originate from the YRV.

The above analyses suggest that there could be positive feedback between the heatwave and the atmospheric circulation through anomalous moisture transportation during the 2022 YRV heatwave. When the YRV heatwave develops, the local evaporation is enhanced and thus produces more atmospheric moisture. The increased atmospheric moisture is further transported to the north of YRV by the high-pressure circulation systems and results in meridional dry air advection over the YRV, which further intensifies the YRV heatwave through the formation of descending motions and associated surface cloud radiative forcing.

4 Conclusion and discussion

The YRV experienced an unprecedented heatwave in midsummer of 2022, with significant global socio-economic and environmental impacts. Although there are existing studies on the mechanisms behind the 2022 YRV heatwave, the previous studies generally assumed that the surface heatwave event was triggered by the overlying atmospheric high-pressure anomalies, and thus predominantly focus on understanding the formation processes of large-scale circulation anomalies in midsummer of 2022. Up to now, there is still insufficient understanding of local feedback processes in the 2022 YRV heatwave.

In this study, we investigated the detailed regional physical processes involved in the influence of atmospheric circulation on the 2022 YRV heatwave. Based on the linearised surface heat budget equation, column-integrated atmospheric moisture flux, and moist static energy equation, the critical processes of the 2022 YRV heatwave are identified. The schematic of the mechanisms responsible for the influence of extreme dry advection on the record-breaking Yangtze River heatwave in midsummer of 2022 is given in Fig. 8. The main conclusions are listed as follows:

(1) The area-averaged SAT anomalies over the YRV in midsummer of 2022 relative to the 1979–2021 climatology is 1.98 °C, which sets the highest record for 1950–2022. The 2022 YRV heatwave is dominated by the component of interannual variability, which contributes 1.44 °C to the total temperature anomalies, accounting for 72.7% of the anomaly amplitude.
(2) Diagnostic analysis based on the linearised surface heat budget equation indicates that the anomalous surface cloud radiative forcing is the most critical process dominating the 2022 YRV heatwave, contributing 2.39 °C to the total anomalies. The anomalous surface cloud radiative forcing is dominated by the positive surface short-wave cloud radiative forcing associated with the negative precipitation anomalies and corresponding decreased cloud cover over the YRV, induced by the vertical dynamical processes of anomalous moisture advection.

(3) Budget analysis of the column-integrated MSE equation for the anomalous vertical velocity over the YRV suggests that the anomalous descending flows are driven by the anomalous meridional dry air advection, which is closely related to the unusually moisture accumulations over the north of YRV. Simulations from the Lagrangian model FLEXPART exhibit that the moisture anomaly over the north of YRV mainly originated from the surface evaporation in the YRV, implying that there could be a positive land-air feedback during the life cycle of the YRV heatwave.

It should be noted that the processes revealed in this study were based on the ERA5 dataset, which not exactly equivalent to the observation. To avoid the possible dataset-dependence of the conclusion, we also utilized the CFSR to conduct the budget analyses. The CFSR can reproduce the main processes in ERA5, including the dominant role of surface short-wave cloud radiative forcing (Fig. S2–S3), the the extreme negative advection of anomalous latent heat energy by climatological meridional wind (anomalous dry air advection) (Fig. S4a–e), and the moisture accumulations over the north of YRV (Fig. S4f). These results suggest that the processes revealed in this study are robust. Whether climate models can reasonably reproduce these physical processes and what impact these physical processes have on the prediction of extreme heat waves deserve further study.

5 Open research

All datasets underlying this study can be downloaded publicly as follows:

(1) ERSSTv5 (https://www.ncei.noaa.gov/products/extended-reconstructed-sst).
(2) ERA5 (https://cds.climate.copernicus.eu/cdsapp#!/dataset/reanalysis-era5-pressure-levels-monthly-means?tab=overview).
(3) CFSR (https://rda.ucar.edu/datasets/ds093.1/ and https://rda.ucar.edu/datasets/ds094-2/).

Supplementary Information The online version contains supplementary material available at https://doi.org/10.1007/s00382-024-07150-0.

Acknowledgements This work is supported by the National Natural Science Foundation of China under Grant No. 42205039, the Guangdong Basic and Applied Basic Research Foundation (2021A1515011421), the Youth Innovation Team of China Meteorological Administration (CMA2023QN15), and the China Postdoctoral Science Foundation under Grant No. 2022T150638.

Funding The authors have not disclosed any funding.

Data availability Enquiries about data availability should be directed to the authors.

Declarations

Conflict of interest The authors declare no conflict of interest.

References

Biasutti M, Voigt A, Boos WR et al (2018) Global energetics and local physics as drivers of past, present and future monsoons. Nat Geosci 11(6):392–400. https://doi.org/10.1038/s41561-018-0137-1

Chen R, Li X (2023) Causes of the persistent merging of the western North Pacific subtropical high and the Iran high during late July 2022. Clim Dyn. https://doi.org/10.1007/s00382-023-06678-x

Choi N, Lee M-I, Cha D-H et al (2020) Decadal changes in the Interannual variability of heat waves in East Asia caused by Atmospheric Teleconnection Changes. J Clim 33(4):1505–1522. https://doi.org/10.1175/jcli-d-19-0222.1

Chou C, Chiang JCH, Lan C-W et al (2013) Increase in the range between wet and dry season precipitation. Nat Geosci 6(4):263–267. https://doi.org/10.1038/ngeo1744

Ding QH, Wang B (2005) Circumglobal teleconnection in the Northern Hemisphere summer. J Clim 18(17):3483–3505. https://doi.org/10.1175/Jcli3473.1

Enomoto T, Hoskins BJ, Matsuda Y (2003) The formation mechanism of the Bonin high in August. Q J R Meteorol Soc 129(587):157–178. https://doi.org/10.1256/qj.01.211

Erdenebat E, Sato T (2018) Role of soil moisture-atmosphere feedback during high temperature events in 2002 over Northeast Eurasia. Progress Earth Planet Sci. https://doi.org/10.1186/s40645-018-0195-4

Ha K-J, Seo Y-W, Yeo J-H et al (2022) Dynamics and characteristics of dry and moist heatwaves over East Asia. npj Clim Atmospheric Sci. https://doi.org/10.1038/s41612-022-00272-4

He C, Zhou T, Zhang L et al (2023) Extremely hot East Asia and flooding western South Asia in the summer of 2022 tied to reversed flow over Tibetan Plateau. Clim Dyn. https://doi.org/10.1007/s00382-023-06669-y

Hersbach H, Bell B, Berrisford P et al (2020) The ERA5 global reanalysis. Q J R Meteorol Soc 146(730):1999–2049. https://doi.org/10.1002/qj.3803

Hu S, Zhou TJ, Wu B (2021) Impact of developing ENSO on Tibetan Plateau Summer Rainfall. J Clim 34(9):3385–3400. https://doi.org/10.1175/Jcli-D-20-0612.1

Jiang J, Liu Y, Mao J et al (2023) Extreme heatwave over Eastern China in summer 2022: the role of three oceans and local soil moisture feedback. Environ Res Lett. https://doi.org/10.1088/1748-9326/acc5fb

Li X, Hu ZZ, Liu Y et al (2023) Causes and Predictions of 2022 Extremely Hot Summer in East Asia. J Geophys Research: Atmos. https://doi.org/10.1029/2022jd038442

Liu B, Zhu C, Ma S et al (2023) Subseasonal processes of triple extreme heatwaves over the Yangtze River Valley in 2022. Weather Clim Extremes. https://doi.org/10.1016/j.wace.2023.100572

Lu J, Cai M (2009) Seasonality of polar surface warming amplification in climate simulations. Geophys Res Lett. https://doi.org/10.1029/2009gl040133

Lu R-Y, Oh J-H, Kim B-J (2002) A teleconnection pattern in upper-level meridional wind over the north African and eurasian continent in summer. Tellus A 54(1):44–55. https://doi.org/10.3402/tellusa.v54i1.12122

Lu R, Xu K, Chen R et al (2023) Heat waves in summer 2022 and increasing concern regarding heat waves in general. Atmospheric Ocean Sci Lett. https://doi.org/10.1016/j.aosl.2022.100290

Ma M, Qu Y, Lyu J et al (2022) The 2022 extreme drought in the Yangtze River Basin: characteristics, causes and response strategies. River 1(2):162–171. https://doi.org/10.1002/rvr2.23

Mallapaty S (2022) China's extreme weather challenges scientists trying to study it. Nature 609(7929):888. https://doi.org/10.1038/d41586-022-02954-8

Neelin JD, Held IM (1987) Modeling tropical convergence based on the Moist Static Energy Budget. Mon Weather Rev 115(1):3–12. https://doi.org/10.1175/1520-0493(1987)115

Peng D, Zhou T, Zhang L (2020) Moisture sources associated with precipitation during dry and wet seasons over central Asia. J Clim 33(24):10755–10771. https://doi.org/10.1175/jcli-d-20-0029.1

Peng D, Zhou T, Sun Y et al (2022) Interannual variation in moisture sources for the First Rainy season in South China estimated by the FLEXPART Model. J Clim 35(2):745–761. https://doi.org/10.1175/jcli-d-21-0289.1

Saha S, Moorthi S, Pan H-L et al (2010) The NCEP climate forecast system reanalysis. Bull Am Meteorol Soc 91(8):1015–1058. https://doi.org/10.1175/2010bams3001.1

Saha S, Moorthi S, Wu X et al (2014) The NCEP climate forecast system version 2. J Clim 27(6):2185–2208. https://doi.org/10.1175/jcli-d-12-00823.1

Seo E, Lee M-I, Schubert SD et al (2020) Investigation of the 2016 Eurasia heat wave as an event of the recent warming. Environ Res Lett. https://doi.org/10.1088/1748-9326/abbbae

Sodemann H, Schwierz C, Wernli H (2008) Interannual variability of greenland winter precipitation sources: lagrangian moisture diagnostic and North Atlantic Oscillation influence. J Phys Res. https://doi.org/10.1029/2007jd008503

Stohl A, Forster C, Frank A et al (2005) Technical note: the Lagrangian particle dispersion model FLEXPART version 6.2. Atmos Chem Phys 5(9):2461–2474. https://doi.org/10.5194/acp-5-2461-2005

Tang S, Qiao S, Wang B et al (2023) Linkages of unprecedented 2022 Yangtze River Valley heatwaves to Pakistan flood and triple-dip La Niña. npj Clim Atmospheric Sci. https://doi.org/10.1038/s41612-023-00386-3

Thompson V, Kennedy-Asser AT, Vosper E et al (2022) The 2021 western North America heat wave among the most extreme events ever recorded globally. Sci Adv 8(18):eabm6860. https://doi.org/10.1126/sciadv.abm6860

Wang W, Zhou W, Chen D (2014) Summer High temperature extremes in Southeast China: bonding with the El Nino-Southern Oscillation and East Asian Summer Monsoon coupled System. J Clim 27(11):4122–4138. https://doi.org/10.1175/jcli-d-13-00545.1

Wang Z, Luo H, Yang S (2023) Different mechanisms for the extremely hot central-eastern China in July–August 2022 from a Eurasian large-scale circulation perspective. Environ Res Lett. https://doi.org/10.1088/1748-9326/acb3e5

Wu B, Zhou T, Li T (2017) Atmospheric dynamic and thermodynamic processes driving the western North Pacific Anomalous Anticyclone during El Niño. Part I: maintenance mechanisms. J Clim 30(23):9621–9635. https://doi.org/10.1175/jcli-d-16-0489.1

Yuan Y, Liao Z, Zhou B et al (2023) Unprecedented hot extremes observed in City clusters in China during Summer 2022. J Meteorological Res 37(2):141–148. https://doi.org/10.1007/s13351-023-2184-9

Zhang D, Chen L, Yuan Y et al (2023) Why was the heat wave in the Yangtze River valley abnormally intensified in late summer 2022? Environ Res Lett. https://doi.org/10.1088/1748-9326/acba30

Zhou TJ, Yu RC (2005) Atmospheric water vapor transport associated with typical anomalous summer rainfall patterns in China. J Geophys Res-Atmospheres. https://doi.org/10.1029/2004jd005413